ACADEMIA ROMÂNĂ
Revue Roumaine de Chimie
http://web.icf.ro/rrch/

Rev. Roum. Chim.,
2019, *64*(5), 433-443
Doi: 10.33224/rrch.2019.64.5.07

SOLID PHASE SYNTHESIS OF FOUR ANALOGS OF AMYLOID-$\beta_{(9-16)}$ PEPTIDE: MS AND FT-IR CHARACTERIZATION

Monica JURESCHI,[a] Ionel HUMELNICU,[a] Brînduşa Alina PETRE,[a,b,*] Cătălina-Ionica CIOBANU,[c] Manuela MURARIU[d] and Gabi DROCHIOIU [a,c,*]

[a] "Al. I. Cuza" University, Faculty of Chemistry, 11 Carol I, Iaşi-700506, Roumania
[b] Center for Fundamental Research and Experimental Development in Translation Medicine – TRANSCEND, Regional Institute of Oncology, 2-4 General Henri Mathias Berthelot, Iaşi-700483, Roumania
[c] Research Department, Faculty of Chemistry, "Al. I. Cuza" University, 11 Carol I, Iaşi-700506, Roumania
[d] Petru Poni Institute of Macromolecular Chemistry, 41a Ghica Vodă Alee, Iaşi-700487, Roumania

Received April 23, 2018

Alzheimer's disease (AD) is the most common cause of dementia and one of its major neuropathological features is the extracellular deposition of fibrils composed of amyloid-β peptides (Aβ). Our investigation started with a small fragment of Aβ, namely the amyloid $A\beta_{(9-16)}$ peptide (^{9}GYEVHHQK^{16}). Here, we report on the synthesis of four new peptides obtained by replacing with glycine or phenylalanine some amino acid residues in the sequence of the above-mentioned $A\beta_{(9-16)}$ peptide, in order to use them to study the oligomerization and fibrillation processes in the presence of metal ions. The following peptides were synthesized by Fmoc/*t*-butyl solid-phase synthesis (SPPS) strategy: $A\beta_{(9-16)}$ (^{9}GYEVHHQK^{16}), $A\beta_{(9-16)}$G (^{9}G^{10}GEVHHQK^{16}), $A\beta_{(9-16)}$F (^{9}G^{10}FEVHHQK^{16}), $A\beta_{(9-16)}$GG (^{9}G^{10}YEV^{13}G^{14}GQK^{16}) and $A\beta_{(9-16)}$GGG (^{9}G^{10}GEV^{13}G^{14}GQK^{16}). The newly synthesized peptides were purified by RP-HPLC and characterized by MALDI-TOF mass spectrometry and Fourier transform infrared spectroscopy (FT-IR) as well as, theoretically, using the GPMAW software. Mass spectrometric spectra confirmed the successful synthesis of the desired peptides, while the hydrophobicity parameter, simulated with the GPMAW software, was shown to be dependent on the structure of each peptide. Infrared spectroscopy showed that the conformation of peptides differs from a peptide to another. Such analogs of $A\beta_{(9-16)}$ peptide fragment are supposed to be of interest in searching the role played by certain amino acids in AD aetiology and, in general, in neurodegeneration.

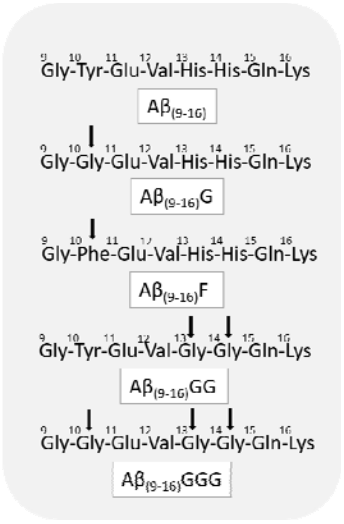

INTRODUCTION

Alzheimer's disease (AD) is the most common neurodegenerative disease and one of the leading causes of death among the old people.[1-7] AD is currently an incurable disorder that affects millions of human beings around the world. About 50% of persons aged 85 or older are at risk for developing this neurodegenerative disease for which currently there is no cure or prevention.[8]

The aggregation of amyloid-β peptides (Aβ), one of the primary pathological hallmarks of AD, plays a key role in the AD pathogenesis. In this regard, Aβ aggregates have been considered as both biomarkers and drug targets for diagnosis and therapy in AD. Various Aβ-targeted metal complexes have exhibited promising potential as anti-AD agents due to their fascinating physicochemical properties over the past two decades.[9,10] The metal-peptide complexes were

* Corresponding authors: gabidr@uaic.ro and brandusa.petre@uaic.ro

classified into three groups based on their potential applications in AD, including therapy, diagnosis and theranosis.[11]

On the other hand, although the etiology of AD is not completely understood, significant evidence showed that the aggregation of Aβ is the pivotal event and causative factor in the occurrence and development of AD. According to the so-called "amyloid cascade hypothesis", the accumulation of Aβ triggers further pathological events, such as dyshomeostasis of metal ions, oxidative stress and mitochondrial dysfunction, as well as hyperphosphorylation of tau and formation of neurofibrillary tangles, resulting in neuronal death and ultimately in AD.[12] The Aβ peptides, produced by proteolytic cleavage of the amyloid precursor protein (APP), have also become a major therapeutic target in AD.[13] Therefore, most experiments aim to reduce the levels of Aβ peptides in the brain. However, the molecular mechanism of Aβ neurotoxicity has not thoroughly been elucidated. Moreover, metal ions such as those of copper, iron and zinc are considered to accelerate the initial formation of amyloid fibril of Aβ peptides.[14,15] In fact, AD is characterized by intracerebral deposition of Aβ, the neurotoxicity being mainly mediated by $A\beta_{(1-40)}$ and especially $A\beta_{(1-42)}$, which are misfolded Aβ peptides found within the AD brain.[3,4,16-18] The 42-amino acid $A\beta_{(1-42)}$ is most toxic, possibly upon self-association into oligomers.[19-21] Nevertheless, it is unclear which amino acid residues are involved in peptide oligomerization. Among the 20 amino acids present in peptides and proteins, only five are electroactive: tyrosine Y, histidine H, methionine M, cysteine C and tryptophan W.[22] However, the hydrophilic N-terminal region of Aβ contains high affinity metal binding sites, particularly the histidine H-rich region of 1–16 residues. In a previous paper, we demonstrated that the 9-16 region is also very active in metal binding.[23] Among the metal coordination sites, the N-terminal histidine residues (His^6, His^{13}, and His^{14}) and several oxygen ligands such as alanine (Ala^2), aspartic acid (Asp^7), glutamic acid (Glu^3, Glu^{11}) and tyrosine (Tyr^{10}) residues have been proposed.[24]

Therefore, this paper aims at presenting the synthesis and characterization of four peptides derived from $A\beta_{(9-16)}$ peptide fragment, in order to study their binding capacity toward heavy metal ions.[23] We have characterized them by mass spectrometry and infrared spectroscopy as well as theoretically with GPMAW software.

RESULTS AND DISSCUSION

Peptide synthesis and characterization

Figure 1 shows the amino acid residues replaced in the native sequence in order to generate the new analogue peptides. The following sequences of peptides were synthesized: 1) H_2N-(Gly-Tyr-Glu-Val-His-His-Gln-Lys)-$CONH_2$ ($A\beta_{(9-16)}$, which is the native sequence); 2) H_2N-(Gly-Gly-Glu-Val-His-His-Gln-Lys)-$CONH_2$ noted as ($A\beta_{(9-16)}G$); 3) H_2N-(Gly-Phe-Glu-Val-His-His-Gln-Lys)-$CONH_2$, for short ($A\beta_{(9-16)}F$); 4) H_2N-(Gly-Tyr-Glu-Val-Gly-Gly-Gln-Lys)-$CONH_2$, in brief ($A\beta_{(9-16)}GG$); and 5) H_2N-(Gly-Gly-Glu-Val-Gly-Gly-Gln-Lys)-$CONH_2$ denominated as ($A\beta_{(9-16)}GGG$), respectively.

All five peptides were manually synthesized on a Rink Amide resin as solid support using the fluorenylmetoxycarbonyl chemistry. After removal from the resin and deprotection, all samples were purified by RP-HPLC chromatography on a C18 column. Depending on the specific hydrophobicity, each peptide eluted at various elution times, as shown in Table 1. For example, $A\beta_{(9-16)}$ eluted at 13.70 min, and $A\beta_{(9-16)}G$ eluted most rapidly at 4.66 min. Thus, the analytical RP-HPLC chromatograms of the five peptides showed major peaks at different retention times, possibly due to their different hydrophobicity degree, which seems to be dependent on each peptide sequence. Individual peaks were selected and each elute was collected and analyzed by MALDI-TOF mass spectrometry.

The structure of the newly synthesized peptides was confirmed by determining their molecular weight on a MALDI-TOF mass spectrometer. We used the MS technique because the MALDI spectrometers have rapidly become one of the most important instruments for peptide and proteins analysis.[25] In addition, this method allows not only the exact determination of molecular weight, but also the purity of peptides.[26] By comparing the theoretical m/z values with the experimental mass spectra (Table 1), it was possible to confirm the successful synthesis of desired peptides. Figure 2 shows the mass spectra of all five $A\beta_{(9-16)}$ peptides. The signals corresponding to the molecular ions ($[M+H]^+$) were observed at m/z 996.83 ($A\beta_{(9-16)}$), m/z 890.81 ($A\beta_{(9-16)}G$), m/z 981.89 ($A\beta_{(9-16)}F$), m/z 836.75 ($A\beta_{(9-16)}GG$), and m/z 730.67 ($A\beta_{(9-16)}GGG$), respectively. In addition to the intact molecular ion signal $[M + H]^+$, there were

also identified two additional peaks characteristic of the adducts with Na^+ and K^+ (Fig. 2). Thus, the characteristic signals at m/z + 22 Da and m/z + 38 Da, where m/z was the molecular ion of $A\beta_{(9-16)}$, were observed at m/z 1018.45 and m/z 1034.43, being attributed to sodium and potassium adducts. The signal for the molecular ion $[M+H]^+$ of $A\beta_{(9-16)}G$ peptide was found at m/z 890.81, whereas the characteristic signal of $[M+Na]^+$ appeared at m/z 912.78, alongside with the signal of $[M+K]^+$ at m/z 928.77. The MALDI-TOF mass spectrum of the peptide $A\beta_{(9-16)}F$ showed the molecular ion $[M+H]^+$ at m/z 981.89, and characteristic signals for $[M+Na]^+$ and $[M+K]^+$ at m/z 1003.87 and m/z 1019.85, respectively. In the case of $A\beta_{(9-16)}GG$ peptide, the molecular ion $[M+H]^+$ was found at m/z 836.75. Similarly, the peaks corresponding to sodium and potassium adducts were also observed at m/z 858.73 and m/z 874.71, respectively. The MALDI-TOF mass spectrum of $A\beta_{(9-16)}GGG$ displayed a peak for the molecular ion $[M+H]^+$ at m/z 730.67 and a signal corresponding to $[M+Na]^+$ ion at m/z 752.65. The theoretical data obtained using the ChemCalc software were consistent with the m/z values obtained with the MALDI-TOF mass spectrometer for all peptides, as shown in Table 2.

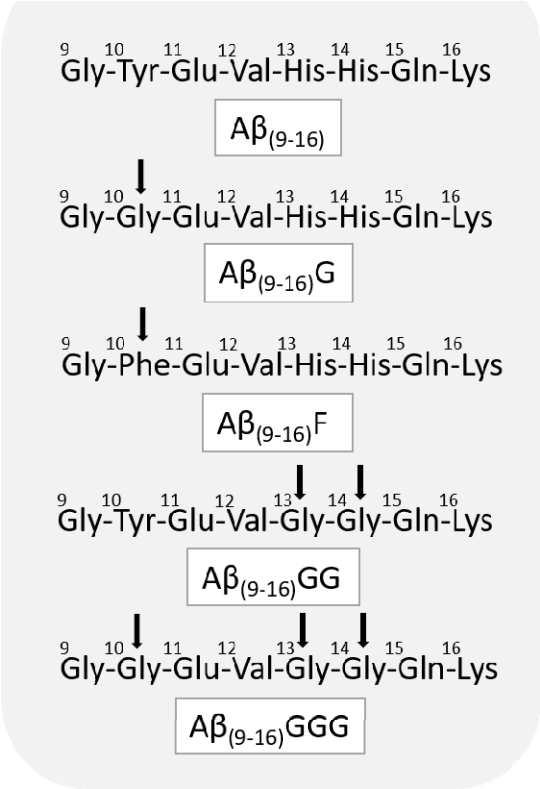

Fig. 1 – General structure of peptides derived from $A\beta_{(9-16)}$.

Table 1

Retention time of peptides analysed by HPLC

Peptide structure	**Peptide abbreviation**	**Retention time (min)**
H_2N-(Gly-Tyr-Glu-Val-His-His-Gln-Lys)-$CONH_2$	$A\beta_{(9-16)}$	13.70
H_2N-(Gly-Gly-Glu-Val-His-His-Gln-Lys)-$CONH_2$	$A\beta_{(9-16)}G$	4.66
H_2N-(Gly-Phe-Glu-Val-His-His-Gln-Lys)-$CONH_2$	$A\beta_{(9-16)}F$	18.52
H_2N-(Gly-Tyr-Glu-Val-Gly-Gly-Gln-Lys)-$CONH_2$	$A\beta_{(9-16)}GG$	14.89
H_2N-(Gly-Gly-Glu-Val-Gly-Gly-Gln-Lys)-$CONH_2$	$A\beta_{(9-16)}GGG$	4.91

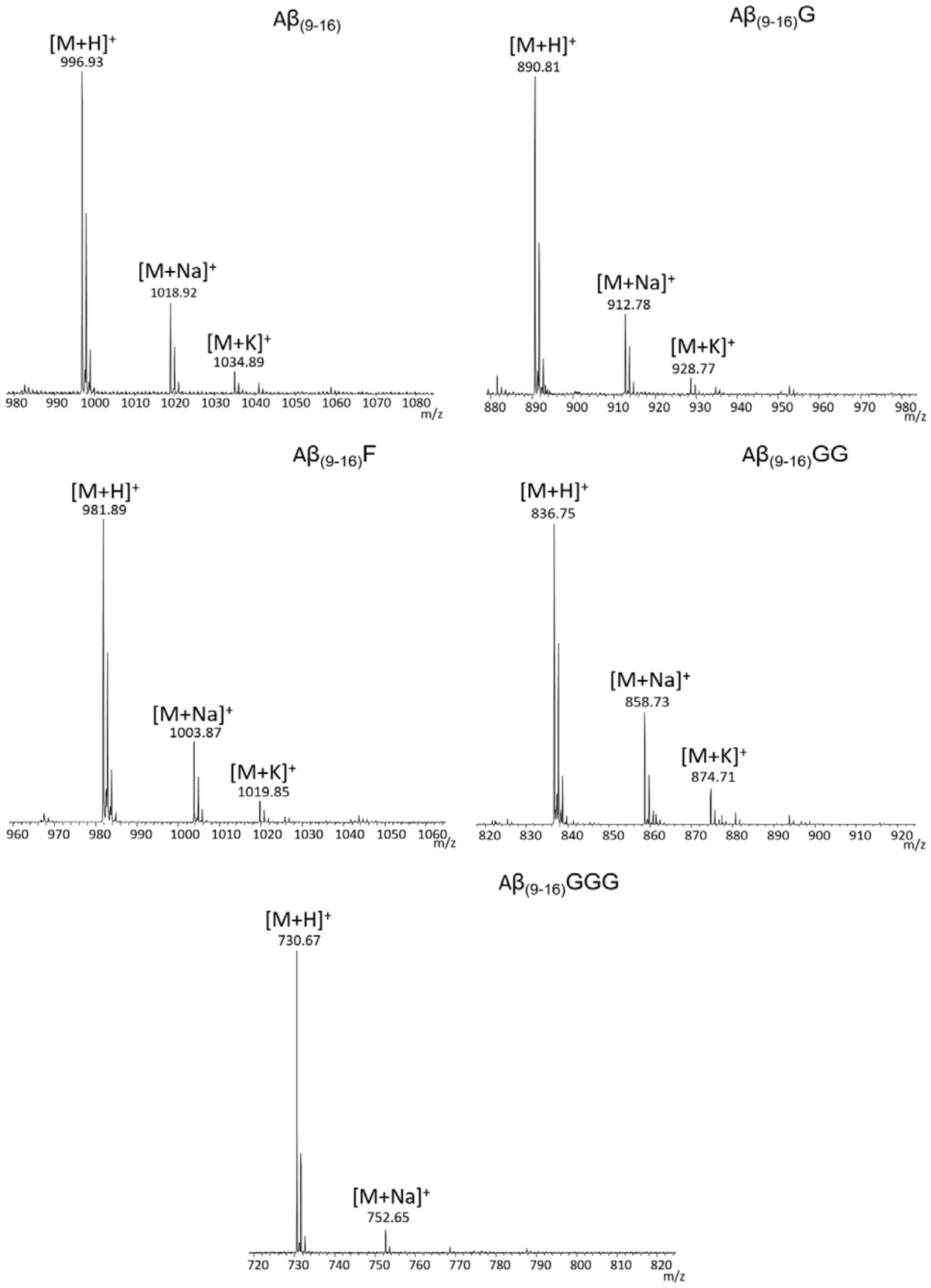

Fig. 2 – MALDI-TOF MS spectra of the newly synthesized analogs of $A\beta_{(9-16)}$ peptide: $A\beta_{(9-16)}$, $A\beta_{(9-16)}G$, $A\beta_{(9-16)}F$, $A\beta_{(9-16)}GG$ and $A\beta_{(9-16)}GGG$, respectively.

Table 2

Molecular weight of the newly synthesized peptides, experimentally determined with a MALDI-TOF instrument and calculated with ChemCalc software

Peptide	Molecular Ion	Theoretical (m/z)	Experimental (m/z)
$A\beta_{(9-16)}$	$[M+H]^+$	996.47	996.93
(H_2N-GYEVHHQK-$CONH_2$)	$[M+Na]^+$	1018.45	1018.92
$C_{44}H_{66}N_{15}O_{12}$	$[M+K]^+$	1034.43	1034.89
$A\beta_{(9-16)}G$	$[M+H]^+$	890.45	890.81
(H_2N-GGEVHHQK-$CONH_2$)	$[M+Na]^+$	912.44	912.78
$C_{37}H_{60}N_{15}O_{11}$	$[M+K]^+$	928.41	928.77
$A\beta_{(9-16)}F$	$[M+H]^+$	981.09	981.89
(H_2N-GFEVHHQK-$CONH_2$)	$[M+Na]^+$	1003.07	1003.87
$C_{44}H_{66}N_{15}O_{11}$	$[M+K]^+$	1019.18	1019.85
$A\beta_{(9-16)}GG$	$[M+H]^+$	836.91	836.75
(H_2N-GYEVGGQK-$CONH_2$)	$[M+Na]^+$	858.89	858.73
$C_{36}H_{56}N_{11}O_{12}$	$[M+K]^+$	875.00	874.71
$A\beta_{(9-16)}GGG$	$[M+H]^+$	730.79	730.67
(H_2N-GGEVGGQK-$CONH_2$)	$[M+Na]^+$	752.77	752.65
$C_{29}H_{52}N_{11}O_{11}$	$[M+K]^+$	768.88	-

FT-IR Study

FT-IR spectroscopy is an analytical technique that can be used to identify compounds and structures using the infrared range of the electromagnetic spectrum. However, the infrared spectra display distinct IR signals for differently folded peptides and proteins. Thus, the peptides have a number of characteristic features in their FT-IR spectra, also called amide bands. Among these, amide bands I and II are the most prominent vibrational bands and are found between the following wavenumber ranges: amide band I (1600-1690 cm^{-1}, C=O stretch), amide II (1480-1575 cm^{-1}, amide III (1229-1301 cm^{-1}, CN stretching, NH bending) are the most commonly used IR bands to disclose conformational changes of proteins and peptides.[27]

The IR spectra of $A\beta_{(9-16)}$ peptides presented in Figure 3A reveal four major peaks in the range from 1800 cm^{-1} to 1000 cm^{-1}. The similarities and differences presented in the spectra are generated especially by the peptide chains and the amino acid residues. For example, in the range 1200-1100 cm^{-1}, characteristic for C–N stretching and C–C–N bending, two important bands were found regardless the type of peptide. Therefore, the $A\beta_{(9-16)}$ peptide, used here for comparison, contains two peaks in the band area at 1194 cm^{-1} and 1133 cm^{-1}, while $A\beta_{(9-16)}G$ peptide where tyrosine (Tyr, Y^{10}) was replaced by glycine (Gly, G^{10}), the two peaks were noticed at 1176 cm^{-1} and 1130 cm^{-1}, respectively. Similar peak was observed at 1164 cm^{-1} and another one at 1133 cm^{-1} in the case of $A\beta_{(9-16)}F$ peptide, where tyrosine (Tyr, Y^{10}) was replaced with phenylalanine (Phe, F^{10}). The $A\beta_{(9-16)}GG$, where the two histidine residues (His, $H^{13,14}$) were modified with two glycine residues (Gly, $G^{13,14}$), two peaks at 1173 cm^{-1} and 1133 cm^{-1} were identified. The $A\beta_{(9-16)}GGG$ peptide, where tyrosine (Tyr, Y^{10}) was replaced by glycine (Gly, G^{10}) and the histidine residues (His, $H^{13,14}$) were replaced by glycine (Gly, $G^{13,14}$) displayed the 1174 cm^{-1} and 1128 cm^{-1} peaks.

The signal for amide I band is produced by the stretching vibrations of the C=O and directly related to the backbone conformation. The native $A\beta_{(9-16)}$ peptide showed two intense peaks at 1627 cm^{-1}, in the amide I band, which are currently thought to correspond to β-sheet conformation and another one around 1662 cm^{-1}, characteristic to random coil structure. The peptide $A\beta_{(9-16)}G$ modified with glycine (Gly^{10}) presented two signals, slightly changed, in comparison with the signals of the native peptide, one at 1625 cm^{-1}, characteristic to β-sheet conformation and another one at 1660 cm^{-1}, characteristic to random coil structure. The peptide $A\beta_{(9-16)}F$ modified with phenylalanine (Phe, F^{10}), displayed also two signals, namely a highly intense one at 1627 cm^{-1}, characteristic to β-sheet conformation and another signal of low intensity at 1657 cm^{-1}, characteristic

to random coil structure. As for the peptide $A\beta_{(9-16)}GG$ containing in its sequence two glycine (Gly, G^{13}, G^{14}) instead histidine, it showed only one intense signal at 1631 cm^{-1}, which corresponds to β-sheet conformation. In the case of glycine rich $A\beta_{(9-16)}GGG$ peptide, (Gly, G^{10}, G^{13}, G^{14}), an intense signal at 1630 cm^{-1} was noticed, which may suggest a β-sheet conformation. In brief, excepting the peptides modified with two or three glycine ($A\beta_{(9-16)}GG$ and $A\beta_{(9-16)}GGG$), which had intense signals at 1631 cm^{-1} and 1630 cm^{-1}, respectively, the other peptides presented two signals, one around 1662-1657 cm^{-1} and another one around 1627-1625 cm^{-1}, which probably is associated with a β-sheet conformation. However, these peptides are too short to be properly characterized conformationally. They are especially of interest for metal binding and less for conformational studies.

The signal for amide II band is related to the N-H bending and C–N stretching in-plane. The investigated peptides showed numerous amide II bands. The native $A\beta_{(9-16)}$ peptide showed a signal at 1534 cm^{-1}, suggesting a β-sheet conformation, while the signal from 1516 cm^{-1} can be safely assigned to tyrosine.[28] Only one peak was seen at 1525 cm^{-1} in the spectra of $A\beta_{(9-16)}G$ and $A\beta_{(9-16)}F$ peptides, which probably can be associated with the β-sheet conformation. The glycine enriched peptides $A\beta_{(9-16)}GG$ and $A\beta_{(9-16)}GGG$ presented a peak at 1514 cm^{-1} and a shoulder of variable intensity at 1534 cm^{-1} that suggest the presence of β-sheet populations and even a possible aggregation.

From the investigation carried out on the amide I and II region from the IR spectrum, important information regarding peptide structure can be obtained. Thus, all peptides may have a large population of β-sheet conformers and a small proportion of random coil structure in the case of $A\beta_{(9-16)}$, $A\beta_{(9-16)}G$ and $A\beta_{(9-16)}F$ peptides. However, since all investigated peptides are formed from only eight amino acids, being thus small peptides, they hardly form stable β-sheet conformation. Consequently, we extended our research on the second derivative of the FT-IR spectra. The second derivative enhances the separation of overlapping peaks and thus offers more specific information than the primary IR absorption spectrum. Therefore, the resolved peaks in the second derivative spectra can be more easily associated to various conformations. As shown in Figure 3B, the second derivative FT-IR spectra of the newly synthesized $A\beta_{(9-16)}$ peptides were evaluated in the range from 1700 to 1600 cm^{-1}. Thus, the signals assigned to β-sheet secondary structure can be easily observed at 1690 cm^{-1} (for the peptides $A\beta_{(9-16)}$, $A\beta_{(9-16)}G$, $A\beta_{(9-16)}F$ and $A\beta_{(9-16)}GG$), at 1648 cm^{-1} (for the peptides $A\beta_{(9-16)}F$, $A\beta_{(9-16)}GG$ and $A\beta_{(9-16)}GG$) and at 1630 cm^{-1} (for the peptides $A\beta_{(9-16)}GG$ and $A\beta_{(9-16)}GGG$). Another signal assigned to β-turns structure was more easily observed at 1675 cm^{-1} in the second derivative spectra of $A\beta_{(9-16)}$ and $A\beta_{(9-16)}G$ peptides. Furthermore, the signal at 1640 cm^{-1} suggested the presence of random coil conformers in the structures of peptides modified with glycine ($A\beta_{(9-16)}GG$ and $A\beta_{(9-16)}GGG$). However, the signal at 1620 cm^{-1} can be assigned to either β-sheet structure and aggregated peptides, being characteristic to $A\beta_{(9-16)}$, $A\beta_{(9-16)}G$ and $A\beta_{(9-16)}F$ peptides. Thus, these peptides were found to form predominantly β-sheet structures. However, since the molecules are small and cannot form complex structures, probably large populations of molecules are random coil or β-sheet. Nevertheless, depending on the chemical structure of each peptide, both the secondary structure and the presence of specific amino acid residues can be revealed in the infrared spectra.

GPMAW study

The GPMAW program provides details about peptides, such as: molecular weight, elemental composition, hydrophobicity, isoelectric point, enzyme cleavage, MS fragmentation etc. The hydrophobicity parameter of the $A\beta_{(9-16)}$ peptide and its analogs, simulated with the GPMAW software, is shown in Figure 4. The native peptide $A\beta_{(9-16)}$ had a higher hydrophilic character compared to all other mutant peptides, due to the tyrosine residue in its sequence, an amino acid whose (-OH) group increases the hydrophilic character of the peptide. In addition, the lower the number of polar groups present in the peptide structure, the lower their hydrophilicity.

Spatial structure of peptides

Using Chem3D Ultra 12.0 software, we calculated the arrangement of molecules in space for the theoretical structures of the peptides represented. The structure of peptides containing more glycine residues seems to be more flexible.

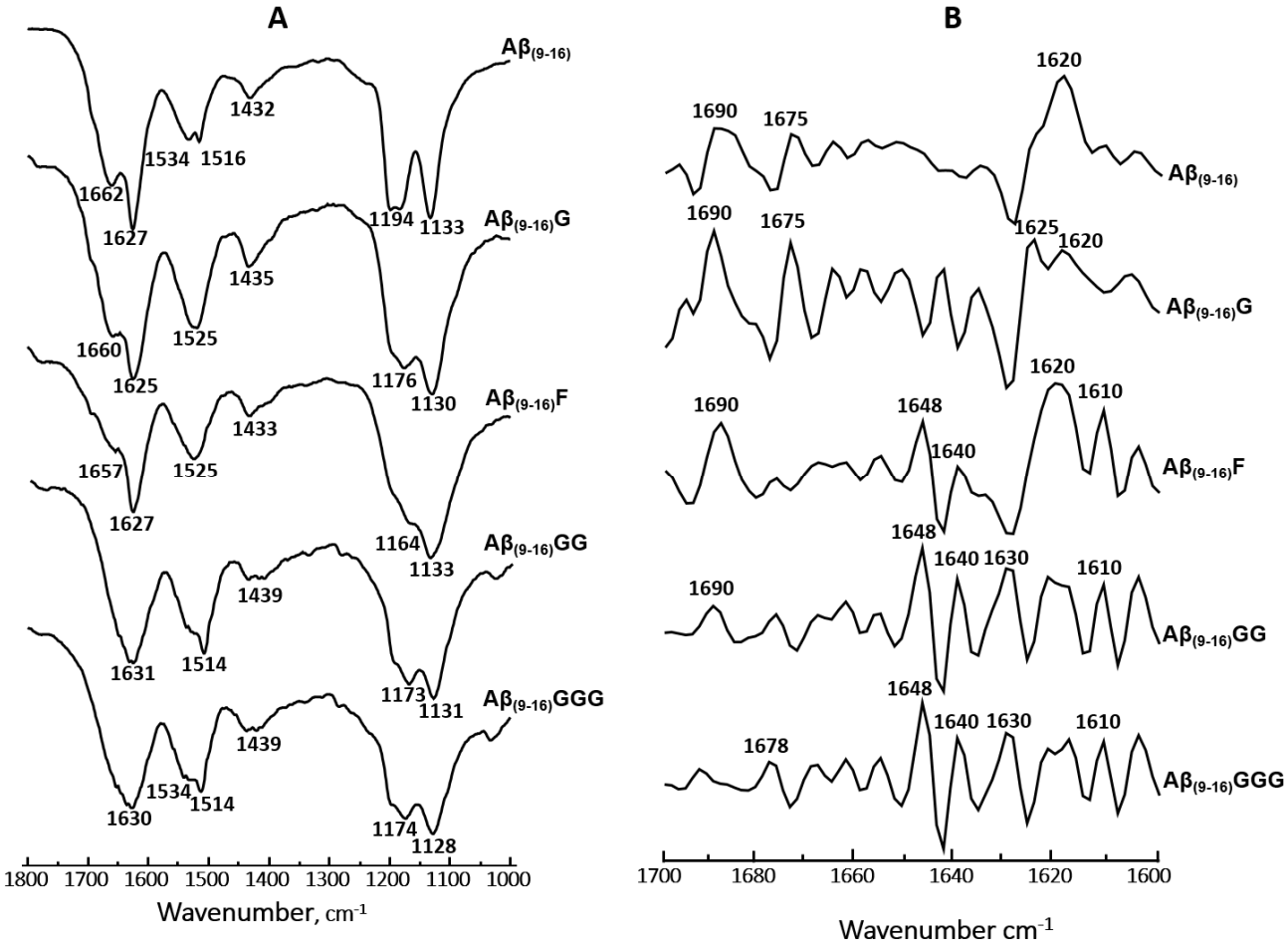

Fig. 3 – FT–IR spectra of the newly synthesized $A\beta_{(9-16)}$-based peptides.

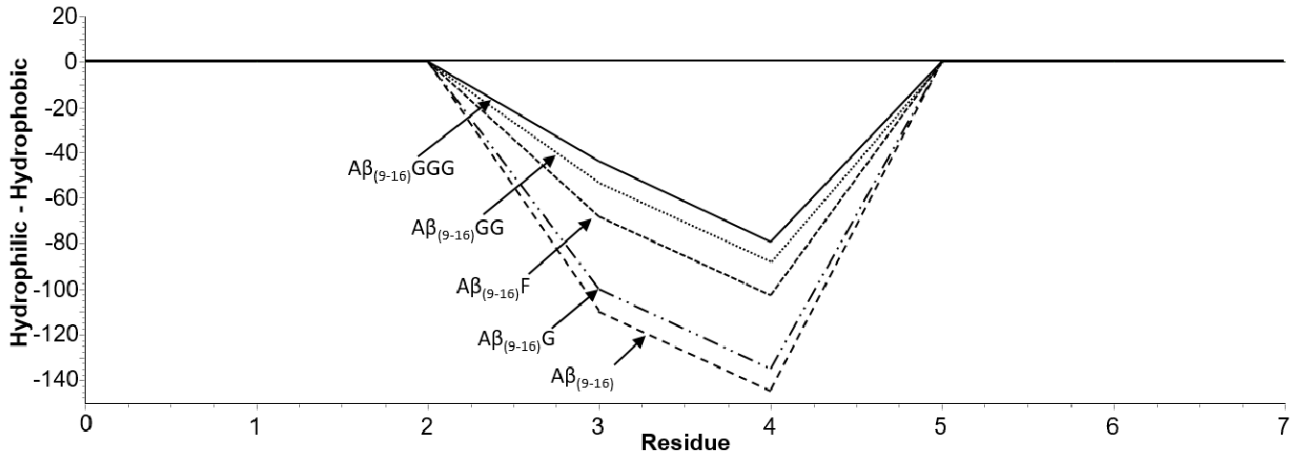

Fig. 4 – Hydrophobicity index of the five Aβ peptides as calculated by the GPMAW software.

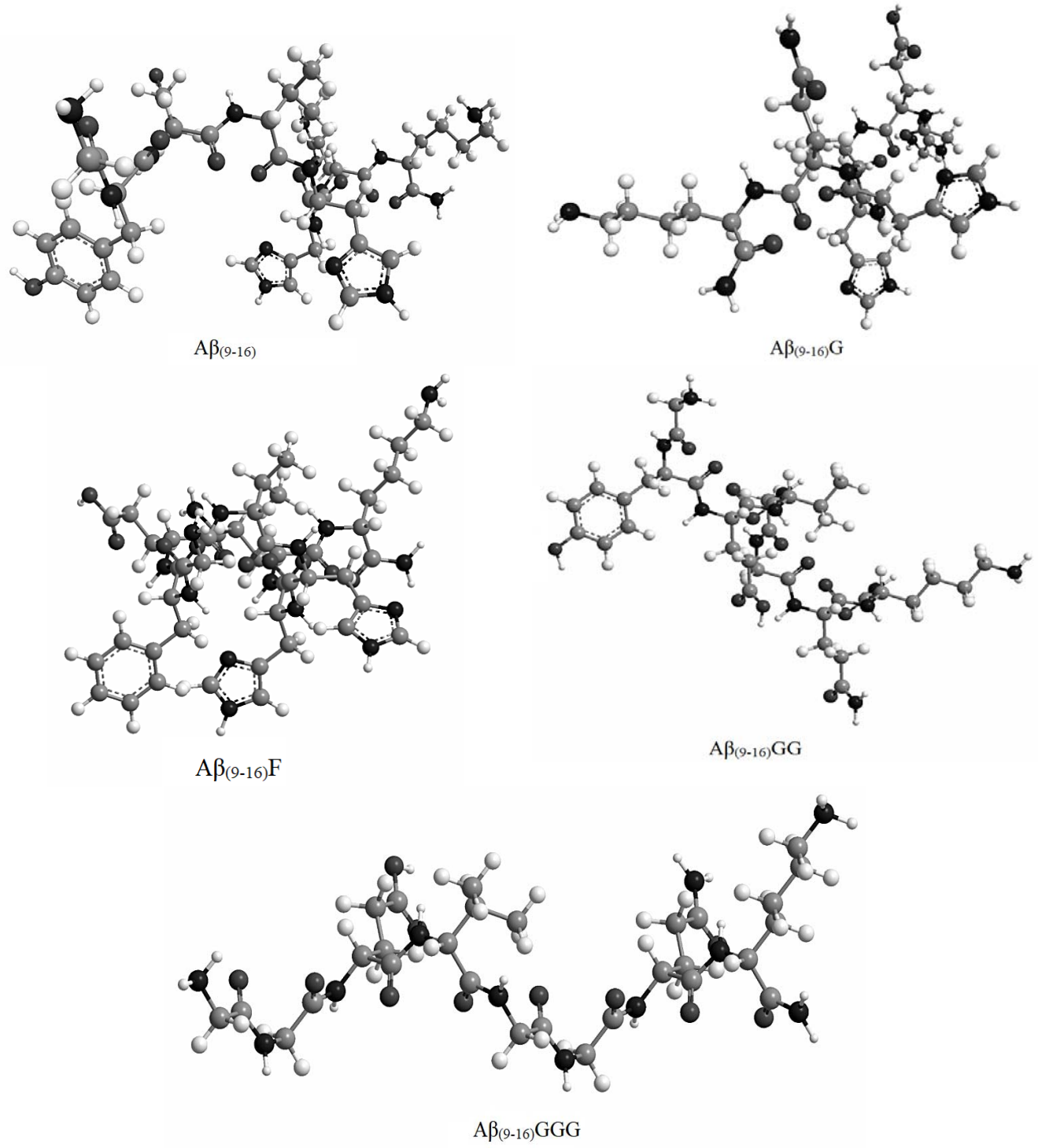

Fig. 5 – Possible spatial structures of $A\beta_{(9-16)}$ analogue peptides as calculated with the ChemDraw Ultra software.

Further research using additional techniques is needed, such as circular dichroism spectroscopy,[29] to monitor changes in the main-chain conformation of these peptides. Previously, a combined technique based on IR, MS and CD spectra was applied to study the conformation of some different histidine-containing peptides.[30]

EXPERIMENTAL

Materials

Peptide synthesis was performed on Rink amide resin with a binding capacity of 0.8-1.0 mmol amino acid/g of resin, purchased from Sigma Aldrich (Fig. 6). The amino acids were protected at the α-amide group with Fmoc (9-fluorenylmethyloxycarbonyl): Fmoc-Lys(Boc)-OH, Fmoc-

Gln(Trt)-OH, Fmoc-His(Trt)-OH, Fmoc-L-Val-OH, Fmoc-Glu(OtBu)-OH, Fmoc-Tyr-(tBu)-OH, Fmoc-L-Gly-OH, Fmoc-L-Phe-OH, and were purchased from GL Biochem (Shanghai). Dimethylformamide (DMF) was obtained from Carl Roth GmbH (Karlsruhe, Germany), while dichloromethane (DCM) and diethyl ether were purchased from Scharlab S.L. (Barcelona, Spain). Piperidine (PYP), 4-methylmorpholine (NMM), triisopropylsilan (TIS), trifluoroacetic acid (TFA), bromophenol blue, ethanol, acetonitrile (ACN) and the activator PyBOP (benzotriazol-1-yl-oxytripyrrolidinophosphonium hexafluorophosphate) were achieved from Merck (Germany), whereas α-cyano-4-hydroxycinnamic acid (HCCA) was purchased from Sigma-Aldrich (Germany). All solutions were prepared using deionized water (18.2 MΩ·cm) from a Milli-Q system (Millipore, Bedford, MA).

Instruments

The obtained peptides were purified using a Dionex UltiMate 3000 UHPLC chromatographic instrument from Thermo Scientific, Bremen, Germany. Separation was performed on a Vydac analytical C18 column of 4.6 mm and a length of 250 mm. Spectrum processing was performed using Chromeleon™ 7.2 Chromatography Data System (CDS).

MALDI-TOF MS analysis was performed on a Bruker Ultraflex MALDI TOF/TOF mass spectrometer operated in positive reflectron mode and equipped with a pulsed nitrogen UV laser (λ_{max} 337 nm). The samples were loaded onto a 384-spot target plate of the MALDI-TOF instrument using the dried-droplet method: the sample and the matrix solution α-cyano-4-hydroxycinnamic acid) were mixed on the target and allowed to dry in the ambient air. The obtained spectra were processed using Bruker´s FlexAnalysis 3.4 software.

FT-IR spectra were recorded with a Bruker Alpha-P FTIR spectrometer (Bruker Optic GmbH, Ettlingen, Germany) equipped with a deuterated triglycine sulphate (DTGS) detector, a temperature-controlled single-bounce diamond attenuated total reflectance (ATR) crystal, and a pressure application device for solid samples. The obtained spectra were processed using Bruker's OPUS software.

Synthesis of the Aβ$_{(9-16)}$ octapeptides

Manual synthesis of peptides by the solid phase method was performed in a fritted plastic syringe. The installation for synthesis was connected to a vacuum pump to remove washing solutions. Peptide synthesis was performed in dimethylformamide (DMF) medium. Protecting groups such as Fmoc or tert-butyl, used to protect the amino acids at the N-terminus or the side chain, were removed with 20% piperidine in DMF.

The following peptides (100 micromoles) were synthesized: H_2N-GYEVHHQK-$CONH_2$ (Aβ$_{(9-16)}$), H_2N-GGEVHHQK-$CONH_2$ (Aβ$_{(9-16)}$G), H_2N-GFEVHHQK-$CONH_2$ (Aβ$_{(9-16)}$F), H_2N-GYEVGGQK-$CONH_2$ (Aβ$_{(9-16)}$GG) and H_2N-GGEVGGQK-$CONH_2$ (Aβ$_{(9-16)}$GGG), respectively. Peptide synthesis was performed manually from the C-terminus of the peptide to the N-terminus by the Fmoc/tBut Solid Phase Synthesis (SPPS) method.

After weighing 125 mg resin, the theoretical amount to synthesize 100 μM peptide, the resin was allowed to swell in the syringe in DMF for 30 min. The first activated amino acid was added after removing the Fmoc protecting groups on the resin with a solution of 20% piperidine in DMF. The deprotection step required the successive replacement of the deprotection solution at 2, 2, 5, 10, 2 and 2 minutes, respectively. Washing was carried out 6 times with a DMF solution.

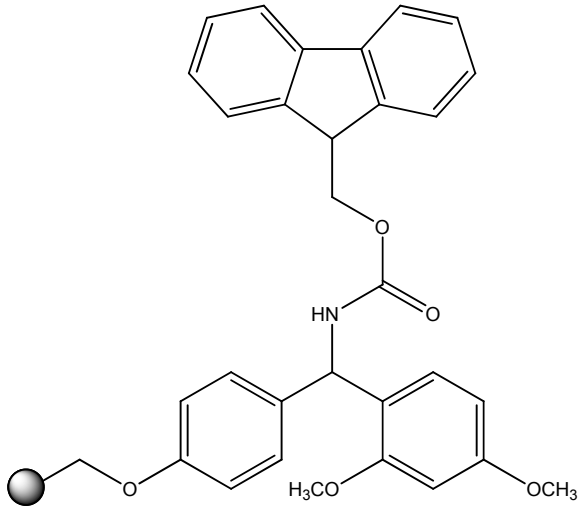

Fig. 6 – Schematic representation of resin Rink amide resin Sigma Aldrich used for peptide synthesis.

Activation of the new amino acid was accomplished by adding of 260 mg of benzotriazol-1-yl-oxytripyrrolidinophosphonium hexafluorophosphate (PyBOP) and 110 μl of N-methylmorpholine (NMM) to the amino acid solution dissolved in DMF. The coupling procedure was performed for 50 minutes to attach each new amino acid. This step was repeated twice in other to achieve a high-efficiency coupling. Each amino acid in the sequence was subjected to the same wash-deprotection-activation cycle.

Finally, the deprotected peptide was washed 6 times with DMF, 3 times with DCM and 3 times with ethanol, then subjected to lyophilization and weighing. Final cleavage of the peptides from the resin was performed in the dark for 3 hours with a TFA: TIS: H_2O solution (95: 2.5: 2.5).

The precipitation of the peptide was performed cold (-20 °C) in a solution of ethyl ether left overnight in the freezer. Collection of fractions required the preparation of a filtration plant consisting of a conical filter bottle, a frit funnel and a rubber stopper, the peptide was removed from the filter by successive washings with a volume of 3 mL of 5% acetic acid solution. The resulting fractions were collected, lyophilized and weighed. Crude products were characterized by analytical RP-HPLC and MALDI-TOF and, when necessary, purified by semipreparative RP-HPLC.

Chromatography

The newly synthesized peptides were purified using a Dionex UltiMate 3000 UHPLC chromatographic instrument from Thermo Scientific, Bremen, Germany. Separation was performed in aqueous-organic medium on a Vydac analytical C18 column of 4.6 mm and a length of 250 mm. The mobile phase used consisted in an aqueous solution of 0.1% TFA in milliQ-grade water (v/v), as solvent A, and 80% ACN, 0.1% TFA in milliQ-grade water (v/v), as solvent B. The peptides (0.1 mg/mL) were dissolved in solvent A, filtered and automatically injected into the chromatographic system. The separation was performed at a flow rate of 1 mL per minute and the UV detector was set at 215 nm, characteristic for the amide bond, while the working temperature was set at 25 °C.

MALDI-TOF mass spectrometry

For MALDI-TOF MS analysis, the samples were co-crystallized with an excess of organic matrix capable to absorb at 337 nm and volatilized under the action of the laser radiation. A saturated solution of α-cyano-4-hydroxy-cinnamic acid (HCCA), used as organic matrix, was dissolved in a solution containing 2: 1 ACN: 0.1% TFA in MilliQ and applied for peptide mapping. Using the dried drop method, that implies first adding of 1 µL of sample and over it 1 µL of freshly prepared matrix solution. Then, the mixture was deposited on a conductive metallic plate called target and allowed to dry. After co-crystallization, the metal plate was introduced into the mass spectrometer and bombarded with short laser pulses. The desorbed and ionized molecules were accelerated by an electrostatic field and discharged through a high-fly metal flight tube. Depending on their mass, the ionized molecules reach the detector at different times, the flight time being in the order of milliseconds.

The spectra were recorded in the positive reflectron mode using the following parameters: 20 kV acceleration voltage, 40% grid voltage, 140 ns delay, low mass gate of 500 Da and an acquisition mass range of 600-3500 Da. A number of 300 shots per acquisition were accumulated to result the final mass spectrum.

External calibration was carried out using the monoisotopic masses of singly protonated ion signals of Bradykinin(1-7) (m/z 757.4), Angiotensin II (m/z 1046.5), Angiotensin I (m/z 1296.7), Substance P (m/z 1347.7), Bombesin (m/z 1619.8), Renin Substrate (m/z 1758.9), ACTH clip(1-17) (m/z 2093.1), ACTH clip(18-39) (m/z 2465.2), and Somatostatin(28) (m/z 3147.5).

FT-IR spectroscopy

The FT-IR spectra of peptides were recorded in solid state on a Bruker Alpha-P FTIR spectrometer (Bruker Optic GmbH, Ettlingen, Germany) equipped with a deuterated triglycine sulphate (DTGS) detector, a temperature-controlled single-bounce diamond attenuated total reflectance (ATR) crystal, and a pressure application device for solid samples. All FT-IR spectra were recorded with a spectral resolution of 2 cm^{-1}, with wavenumber accuracy of 0.01 cm^{-1}. Processing of the FT-IR data was performed using the Bruker OPUS software.

Computer programs

Confirmation of the peptide structure was possible by comparing the signals obtained in the mass spectra with the theoretical ones, calculated using the application web ChemCalc.[31] The same information can be obtained using the General Protein Mass Analysis for Windows (GPMAW, Lighthouse Data, Denmark) program. Besides, this soft is capable to generate a hydrophobicity graph characteristic to the studied peptide.[32] Computer simulation was done with the Chem3D Ultra 12.0 program.[33]

CONCLUSIONS

Here, we have synthesized four new mutant peptides derived from the $A\beta_{(9-16)}$ peptide fragment. Both the native peptide and its analogs were characterized by MALDI-TOF mass spectrometry and Fourier transform infrared spectroscopy (FT-IR). Both mass spectrometry and infrared spectroscopy confirmed the new sequences of the peptides. The peptides were also investigated using the GPMAW software, which revealed that the peptide $A\beta_{(9-16)}$ has a higher hydrophilic character compared to all the other investigated peptides, probably due to the tyrosine residue in its sequence, whose hydroxyl group increases its hydrophilic character. Computer simulation was done with the Chem3D Ultra 12.0 software, which suggested that the structure of peptides containing more glycine residues is more flexible. New research is needed to find other important properties of the newly synthesized peptides, followed by their interaction with metal ions.

Acknowledgements: Funding from Roumanian Government (UEFISCDI Bucharest, PN-III-P4-ID-PCE-2016-0376, Contract 56/2017) is gratefully acknowledged.

REFERENCES

1. P. Wang and Z. Y. Wang, *Ageing Res. Rev.*, **2017**, *35*, 265-290.
2. A. Terracciano and A. R. Sutin, *Personal Disord.*, **2019**, *10*, 4-12.
3. C. Haass, M. G. Schlossmacher, A. Y. Hung, C. Vigo-Pelfrey, A. Mellon, B. L. Ostaszewski, I. Lieberburg, E. H. Koo, D. Schenk, D. B. Teplow, and D. J. Selkoe, *Nature*, **1992**, *359*, 322-325.
4. M. Shoji, T. E. Golde, J. Ghiso, T. T. Cheung, S. Estus, L. M. Shaffer, X. D. Cai, D. M. McKay, R. Tintner and B. Frangione, *Science*, **1992**, *258*, 126-129.
5. P. Seubert, C. Vigo-Pelfrey, F. Esch, M. Lee, H. Dovey, D. Davis, S. Sinha, M. Schiossmacher, J. Whaley, C. Swindlehurst and R. McCormack, *Nature*, **1992**, *359*, 325-327.
6. C. S. Atwood, R. C. Scarpa, X. Huang, R. D. Moir, W. D. Jones, D. P. Fairlie, R. E. Tanzi and A. I. Bush, *J. Neurochem.*, **2008**, *75*, 1219-1233.
7. A. Veloso and K. Kerman, *Anal. Bioanal. Chem.*, **2013**, *405*, 5725-5741.
8. X. Wang, X. Wang, and Z. Guo, *Coord. Chem. Rev.*, **2018**, *362*, 72-84.
9. D. D. Carlton, and K. A. Schug, *Anal. Chim. Acta*, **2011**, *686*, 19-39.
10. E. Farkas, and I. Sóvágó, *Amino Acids, Pept. Proteins*, **2012**, *37*, 66-118.
11. H. Liu, Y. Qu, and X. Wang, *Future Med. Chem.*, **2018**, *10*, 679-701.
12. E. Karran, M. Mercken and B. De Strooper, *Nat. Rev. Drug Discov.*, **2011**, *10*, 698-712.
13. C. A. Lemere, and E. Masliah, *Nat. Rev. Neurol.*, **2010**, *6*, 108-119.
14. H. NisHizawa, and H. Okumura, *J. Comput. Chem. Jpn.*, **2018**, *17*,76-79.
15. G. Di Natale, F. Bellia, M. F. Sciacca, T. Campagna, and G. Pappalardo, *Inorg. Chim. Acta*, **2018**, *472*, 82-92.
16. Y. Huang, and L. Mucke, *Cell,* **2012**, *148*, 1204-1222.
17. D. J. Selkoe, *Cold Spring Harb. Perspect. Biol.*, **2011**, *3*, a004457-a004457.

18. P. Seubert, C. Vigo-Pelfrey, F. Esch, M. Lee, H. Dovey, D. Davis, S. Sinha, M. Schiossmacher, J. Whaley, C. Swindlehurst and R. McCormack, *Nature*, **1992**, *359*, 325-327.
19. C. J. Pike, A. J. Walencewicz, C. G. Glabe and C. W. Cotman, *Brain Res.*, **1991**, *563*, 311-314.
20. C. Geula, M. M. Mesulam, D. M. Saroff, and C. K. Wu, *J. Neuropathol. Exp. Neurol.* **1998**, *57*, 63-75.
21. G. M. Shankar, S. Li, T. H. Mehta, A. Garcia-Munoz, N. E. Shepardson, I. Smith, F. M. Brett, M. A. Farrell, M. J. Rowan, C. A. Lemere and C. M. Regan, *Nat. Med.*, **2008**, *14*, 837-842.
22. T. A. Enache, A. M. Chiorcea-Paquim and A. M. Oliveira-Brett, *Anal. Chem.*, **2018**, *90*, 2285-2292.
23. M. Murariu, L. Habasescu, C. I. Ciobanu, R. V. Gradinaru, A. Pui, G. Drochioiu and I. Mangalagiu, *Int. J. Pept. Res. Ther.,* **2019**, 1-13.
24. S. T. Mutter, M. Turner, R. J. Deeth and J. A. Platts, *ACS Chem. Neurosci.*, **2018**, *9*, 2795-2806.
25. M. Dashtiev, E. Wäfler, U. Röhling, M. Gorshkov, F. Hillenkamp and R. Zenobi, *Int. J. Mass. Spectrom.*, **2007**, *268*, 122-130.
26. W. Sandoval, *Curr. Protoc. Protein*, **2014**, *77*, 16.2.1-16.2.11.
27. J. Kong, and S. Yu, *Acta Biochim. Biophys. Sin.*, **2007**, *39*, 549-559.
28. E. Goormaghtigh, J. M. Ruysschaert, and V. Raussens, *Biophys. J.*, **2006**, *90*, 2946-2957.
29. M. Murariu, K. Popa, E. S. Dragan, G. Drochioiu, *Rev. Roum. Chim*., **2009**, *54*, 741-747.
30. M. Murariu, E. S. Dragan, G. Drochioiu, *Int. J. Pept. Res. Ther*., **2009**, *15*, 303-311.
31. L. Patiny and A. Borel, *J. Chem. Inf. Model*, **2013**, *53*, 1223-1228.
32. S. Peri, H. Steen and A. Pandey, *Trends Biochem. Sci.,* **2001**, *26*, 687-689.
33. D. A. Evans, *Angew. Chem. Int. Ed.*, **2014**, *53*, 11140-11145.